cosmetics

MDPI

Article

Unveiling the Potential of Plant-Derived Exosome-like Extracellular Vesicles from *Phalaenopsis aphrodite* as Skin-Conditioning Ingredients in Cosmetic Applications

Kai-An Chuang [1,2], Kuei-Chang Li [1,2], Hsin-Jan Yao [1,2], Pei-Yin Tsai [1,2], I Huang Lu [3], Chu Hung Lin [3], Hira Umbreen [4], Chi-Chien Lin [5] and I-Hong Pan [1,2,*]

1 Advanced Product R&D Center, Pegavision Corp., Hsinchu City 300, Taiwan; andychuang@facial-beau.com (K.-A.C.)
2 FacialBeau International Corp., New Taipei City 242, Taiwan
3 Biomedical Technology and Device Research Laboratories, Industrial Technology Research Institute, Hsinchu 300, Taiwan
4 Institute of Biomedical Science, The iEGG and Animal Biotechnology Center, National Chung-Hsing University, Taichung 402, Taiwan
5 Institute of Biomedical Science, National Chung-Hsing University, Taichung 402, Taiwan
* Correspondence: joycepan@facial-beau.com; Tel.: +886-3-575-0250

Abstract

Plant-derived exosome-like extracellular vesicles (PELVs) have recently emerged as novel bioactive materials. Although members of the Orchidaceae family have been reported to possess various biological activities and are widely used as cosmetic ingredients, no studies to date have investigated exosome-like extracellular vesicles derived from *Phalaenopsis* species. In the present study, we report for the first time a novel exosome-like extracellular vesicles preparation isolated from *Phalaenopsis aphrodite* (called Exorigin® OR) and characterize its physical and biological properties. The purified vesicles exhibited a spherical shape surrounded by a bilayered membrane with an average particle size of approximately 98 nm and expressed a CD9 marker. Fluorescent labeling with BODIPY TR indicated that Exorigin® OR can be internalized by cells. In in vitro assays, Exorigin® OR alleviated hydrogen peroxide-induced damage in keratinocytes and inhibited melanin production in melanocytes, possibly associated with the downregulation of *Tyrp1* expression as shown by qPCR analysis. Moreover, reconstructed human epidermis and cornea-like epithelium models demonstrated that Exorigin® OR is non-irritant. Collectively, these findings suggest that Exorigin® OR represent a promising and safe bioactive ingredient for promoting skin health in cosmeceutical applications.

Keywords: *Phalaenopsis aphrodite*; exosome-like extracellular vesicles; plant-derived exosomes; cell protection; anti-melanogenesis; cosmetic

Check for updates

Academic Editor: Enzo Berardesca

Received: 3 December 2025
Revised: 24 December 2025
Accepted: 9 January 2026
Published: 12 January 2026

Copyright: © 2026 by the authors. Licensee MDPI, Basel, Switzerland. This article is an open access article distributed under the terms and conditions of the Creative Commons Attribution (CC BY) license.

1. Introduction

Plant-derived exosome-like extracellular vesicles (PELVs) are a type of natural active substance, typically ranging from 50 to 500 nm in diameter [1]. They have been widely reported recently due to their potential health benefits and new biomedical applications. PELVs have similar structures to mammalian exosomes with a diverse class of lipid-rich bilayer membrane [2] and contain diverse bioactive molecules, including proteins, lipids, nucleic acids and secondary metabolites [3]. These particles play a crucial role in regulating plant physiology and mediating processes such as nutrient transport, stress response,

cellular signaling, and growth modulation. They have been reported to be able to come from fruits, vegetables, and Chinese herbal medicine [3–6]. Research has also found that PELVs can enter human cells, demonstrating the possibility of cross-species biological activity [7].

The skin is the largest organ in the body, covering its entire external surface. It serves as a chemical, physical, and immune barrier between the internal and external environments [8]. Because of the barrier function, it limits the absorption and penetration of molecules or peptides into the skin, hindering their skin care effects [9]. However, many studies have shown that plant vesicles have good dermal bioavailability, and they may have great potential application for delivery systems in cosmetic industries [10]. For example, study has shown that plant-derived exosomes (pExo) from broccoli can efficiently penetrate through the stratum corneum (SC) of porcine skin layers by Franz diffusion experiment [11]. Using plant exosomes as cargo to encapsulate resveratrol has been found to have multi-faceted improvements in human skin, highlighting its application in skin care [12]. It is currently known that there are generally two pathways for transdermal permeation of PELVs, including the transfollicle pathway and penetration through the stratum corneum, which can be divided into transcellular and intercellular pathways [13]. In addition, compared with animal sources, PELVs highlight their advantages due to their stable productive source, minimal safety concerns, low immunogenicity, and environmentally friendly properties [14]. We therefore consider that PELVs have significant application value in cosmetic raw materials.

Taiwan is known as the "Island (or Kingdom) of orchids" and one of the world's orchid cultivation and hybridization centers. The excellent quality of Taiwan's hybrid varieties has attracted consumers from all over the world. Orchids are plants that belong to the family Orchidaceae, which is the largest family of flowering plants, with an estimated 17,000 to 35,000 different wild species [15]. Among these Orchids, *Phalaenopsis* accounts for the largest proportion of Taiwan's exports value due to its beauty as an ornamental flower. For example, the most well-known species *Phalaenopsis aphrodite*, also called "Taiwanese Grandma", is characterized by pure white flowers. Orchid plants have been used as traditional Chinese medicine in China for a long time [16]. In addition to their medicinal uses, orchids have now been expanded to the cosmetic industries [15]. Many companies use orchid extracts as an ingredient in product development. Research shows that phytoconstituents from *Vanda teres* modulate mitochondrial activity through stimulation of cytochrome c oxidase and impart anti-aging effect to human keratinocytes [17]. The extract of *Vanda coerulea* displayed DPPH radical scavenging activity and inhibitory effect of PGE-2 in irradiated HaCaT cells [18], even though its extract may possess skin hydrating effect by stimulating the expression of aquaporin 3 (AQP3), which plays an important role in water and glycerol transport between cells [19]. Although the above studies provide insights into the potential use of orchid extracts as a cosmetic active ingredient, there is currently a lack of scientific research on PELVs from orchid plants, particularly *P. aphrodite* in which we are interested. To the best of our knowledge, most research on *P. aphrodite* focuses on morphology, physiology, gene expression, disease resistance, reproductive mechanisms, and other aspects, and explores its applications in horticulture and biology [20–24]. More specifically, little is known about the biological effects of PELVs from *P. aphrodite*.

In the present study, we report a novel exosome-like extracellular vesicle preparation derived from *P. aphrodite* (called Exorigin® OR), whose biological activities were investigated using in vitro models in HaCaT and B16-F0 cell lines. We characterized the particle size, transmission electron microscopy morphology, and surface markers of EVs. Furthermore, Exorigin® OR was internalized by keratinocyte cells and exerted cell-protective activity. We also revealed that Exorigin® OR can suppress melanogenesis, potentially

through pathways related to melanin metabolism. In addition, reconstructed skin models confirmed the safety of Exorigin® OR. Collectively, our study highlights the potential application of Exorigin® OR as cosmetic ingredients.

2. Materials and Methods

2.1. Chemicals and Reagents

The 3-isobutyl-1-methylxanthine (IBMX), hydrogen peroxide solution (H_2O_2) and L-tyrosine were purchased from Uni-onward (New Taipei City, Taiwan). Thiazolyl Blue Tetrazolium Bromide (MTT) was from BioPioneer Tech CO., Ltd. (New Taipei City, Taiwan).

2.2. Isolation and Purification of Exosome-like Extracellular Vehicles (EVs)

Briefly, *P. aphrodite* (White flower) was purchased from Tai-Ling Biotech Inc. in Taiwan. The plant materials (Flower and Pedicel) were crushed and homogenized by using a blender in a weight ratio of 1:1.5 (*w*/*w*) with phosphate-buffered saline (PBS), and the filtered juice was serially centrifuged at 8000 rpm for 30 min to remove large debris. After centrifugation, the supernatant was filtered through a tangential flow filtration (TFF) system (AKTA flux 6, Cytiva, Marlborough, MA, USA) with 0.22 µm hollow fiber membranes (CFP-2-E-4X2MA, Cytiva). Then, the filtrate was isolated and concentrated using tangential filter with 100 kD cut-off hollow fiber membranes (UFP-100-C-4X2MA, Cytiva). The final TFF filtration (called Exorigin® OR) was concentrated about 10 times and then analyzed.

2.3. Quantification and Size Assessment of Exorigin® OR

Exorigin® OR was eluted by the size-exclusion chromatography; (SEC-eluted EVs) are enriched and purified via the qEV Isolation platform (Automatic Fraction Collector V2, Izon Science, Christchurch, New Zealand) [25]. The procedure was performed in accordance with the manufacturer's instructions. After cleaning and equilibrating the qEV column (pore size 70 nm) with filtered PBS, TFF filtrate was applied on the top of the column and the fraction was eluted by PBS. Then, the size distribution and the particle concentration of the isolated fraction was analyzed via Tunable Resistive Pulse Sensing (TRPS) measurements with the Exoid instrument mounting a polyurethane nanopore membrane NP200 (Izon Science, New Zealand).

2.4. Transmission Electron Microscopy (TEM)

The visualization of Exorigin® OR was using transmission electron microscope (TEM) [26]. Briefly, the sample was dropped onto a carbon-coated copper grid. Excess liquid was removed by filter paper. Then, the sample was negatively stained with 2% Uranyl acetate. Excess stain solution was removed using a filter paper, and the sample was air-dried. Finally, the sample was imaged using HT-7700 transmission electron microscope (Hitachi, Tokyo, Japan) with an operating voltage of 100 kV.

2.5. CD9 Marker Detection

The presence of tetraspanin marker CD9 was detected using the ExoELISA-ULTRA Complete Kit (System Biosciences, Palo Alto, CA, USA) according to the manufacturer's instructions [27]. The SEC-eluted EVs were diluted in exosome binding buffer and used for marker detection. The absorbance was measured at 450 nm using Synergy H1 multi-mode plate reader (Agilent Technologies, Winooski, VT, USA).

2.6. Cell Culture

Human HaCaT keratinocytes and mouse B16-F0 melanocyte cell line were obtained from iCell Bioscience Inc. (iCell Bioscience, Shanghai, China) and Bioresource Collection

and Research Center (BCRC, Hsinchu City, Taiwan), respectively. Both cells were cultured in high glucose Dulbecco's modified Eagle's medium (DMEM, Thermo Fisher Scientific, Waltham, MA, USA) supplemented with 10% fetal bovine serum, 100 units/mL of penicillin, and 100 µg/mL of streptomycin and kept at 37 °C in a humidified incubator at 5% CO_2. For cell subculture, both cell types were treated with 0.25% trypsin for digestion when they reached the logarithmic growth phase. Next, culture medium was added to terminate the digestion reaction, and the cells were centrifuged at 500× *g* for 5 min to remove the trypsin. The cell concentrations were then adjusted to 1×10^5/mL for HaCaT cells and 5×10^4/mL for B16-F0 cells by adding an appropriate volume of medium [28,29].

2.7. Cell Viability Assay

The cytotoxicity of Exorigin® OR was performed by MTT assay [29]. HaCaT (10^4 cells/well) was seeded in culture plate and incubated at 37 °C in 5% CO_2 for 24 h. Then, the cells were treated with Exorigin® OR for 24 h. For the B16-F0 cell, the cell treatment procedure and duration were the same as those used in the melanin induction assay. After incubation, the medium was discarded and MTT reagent was added into each well (final concentration of 0.5 mg/mL) and incubated for 2 h at 37 °C. After reaction, DMSO was added to solubilize the formazan crystals. The optical density of the formazan crystals was measured at 570 nm absorbance using Synergy H1 multi-mode plate reader. The optical density control group was evaluated 100% alive and Exorigin® OR-treated groups were compared to control.

2.8. Labeling and Assessment of the Interaction Between Exorigin® OR and Cells

EVs were stained with BODIPY® TR Ceramide (Thermo Fisher Scientific) by the characterization of lipid bilayer [30]. Briefly, the SEC-eluted EVs were labeled with 1 µM of BODIPYTM TR Ceramide for 1 h at 37 °C. Excess dye was removed using Amicon® Ultra Filters (Merck Millipore Ltd., Billerica, MA, USA) with a molecular weight cut-off (MWCO) of 100 kDa by 1X PBS. HaCaT cells (10^4 cells/well) were prepared for cell uptake assay before staining. After overnight incubation in black polystyrene 96-well microplates, labeled EVs were added into cells for another 24 h in complete culture medium. After that, the medium was removed and cells were washed three times with culture medium to remove free-labeled EVs. Finally, the uptake of labeled EVs was recorded using the BioTek Lionheart FX microscope under live-cell imaging events (Agilent Technologies, Inc.).

2.9. Keratinocyte Injury Assay

MTT assay was applied to determine the cell viability of Exorigin® OR against the oxidative stress effect induced in HaCaT cells by H_2O_2 exposure [29]. HaCaT cells were seeded at a density of 10^4 cells/well in a 96-well culture plate and incubated at 37 °C in 5% CO_2 for 24 h. Then, cells were pre-treated Exorigin® OR in the concentrations range from 2.5% to 10% (*v*/*v*) for 30 min before the oxidative damage. After exposure to H_2O_2 (200 µM), cells were cultured in 5% CO_2 incubator at 37 °C for 24 h. Finally, recovery of cell viability was analyzed by the MTT method as described above or stained with Sirius red. The optical density control group was evaluated 100% alive and Exorigin® OR and H_2O_2-treated groups were compared to control.

2.10. Melanin Induction and Content Assay

Melanin content was evaluated by cell-based induction assay based on the method described previously with minor modifications [31]. B16-F0 cells (5×10^3/well) were seeded in 6-well plates with complete culture medium and incubated for 24 h. Next, the medium was replaced with medium containing 72 µg/mL of l-tyrosine and added various concentrations of Exorigin® OR and IBMX (100 µM) to final concentrations for 96 h. For

the detection of intracellular melanin, each group of cells was harvested by centrifugation at 500× *g* for 5 min with 96-well round bottom plate and washed cell pellet with 1X PBS. After repeated centrifugation, cell pellets were photographed using a digital camera, then dissolved in 1.0 N NaOH containing 10% DMSO, heated at 80 °C for 30 min. Finally, the absorbance at 405 nm was measured via the Synergy H1 multi-mode plate reader (Agilent Technologies). The control group of melanin content was defined as 100%.

2.11. Quantitative Real-Time PCR

Total RNA was purified using a PureLink RNA Mini Kit (Invitrogen, Carlsbad, CA, USA). The concentration was then measured using Synergy H1 multi-mode plate reader with the BioTek's Take3 Multi-Volume Plate. The RNA purity was determined by the A260/A280 ratio. Purified total RNA (1 μg) was subjected to cDNA synthesis using a RevertAid RT Reverse Transcription Kit (Thermo Fisher Scientific, Waltham, MA, USA). Gene expression was measured with a Bio-Rad CFX Duet Real-Time PCR System using the KAPA SYBR FAST universal 2× qPCR master mix and primers ordered from Protech Technology Enterprise (Taipei, Taiwan). Glyceraldehyde-3-phosphate dehydrogenase (*Gapdh*) was used as a normalization control. All results were calculated using the $2^{-\Delta\Delta Ct}$ method and normalized to GAPDH. The sequences of primers used are shown in Table 1. Primers were selected based on sequences provided by OriGene Technologies Inc. (Rockville, MD, USA) as well as those reported in the literature [32,33]. Primer specificity was validated using the on-line Primer-BLAST tool available on the NCBI website.

Table 1. Sequences of primers used for real-time PCR.

Gene	Forward Primer (5′-3′)	Reverse Primer (5′-3′)
mGapdh	CATCACTGCCACCCAGAAGACTG	ATGCCAGTGAGCTTCCCGTTCAG
mTyr	CAGGCTCCCATCTTCAGCAGAT	ATCCCTGTGAGTGGACTGGCAA
mMitf	GATCGACCTCTACAGCAACCAG	GCTCTTGCTTCAGACTCTGTGG
mTyrp1	ATGGAACGGGAGGACAAACC	TCCTGACCTGGCCATTGAAC

2.12. In Vitro Skin and Eye Irritation

The safety evaluation of Exorigin® OR was conducted by an independent third-party research institute (SGS, New Taipei City, Taiwan). In accordance with the methodology recommended by the manufacturer, irritation studies were performed on reconstructed human epidermis (EpiSkin™, Lyon, France) and reconstructed human cornea-like epithelium models (J-TEC) to assess potential skin and eye irritation. The assessment criteria followed the UN Globally Harmonized System (GHS) No category, whereby a cell viability of ≤50% was classified as skin irritation, and a cell viability of ≤40% was classified as eye irritation.

2.13. Statistical Analysis

All data in this study are presented as mean ± standard deviation. One-way ANOVA with Dunnett's multiple comparisons test was used to determine the level of significance. Statistical significance was defined as p-value < 0.05.

3. Results

3.1. Characterization of Exorigin® OR

To assess the concentration, size, and morphology of Exorigin® OR, SEC-eluted EVs were subjected for experiments by Exoid and TEM, which are identification methods recommended by MISEV2023 [34]. The yield of Exorigin® OR was 5.51 × 10^9 particles/mL. The particles are nanosized, and the average diameter of the particle population is 98 nm (Figure 1a). TEM result showed that Exorigin® OR was spherical and surrounded by a

plasmatic membrane corresponding to the vesicular topology (Figure 1b). Previous studies have demonstrated that the CD9 tetraspanin protein exhibits a conserved structural similarity between plants and animals and is present in plant-derived extracellular vehicles [35,36]. To confirm the characteristics of Exorigin® OR, we used different amounts of SEC-eluted particles to detect CD9 surface markers using ELISA. The results found that the EVs have a dose-dependent detection signal ($p < 0.0001$), compared to the blank (Figure 1c). To further examine whether Exorigin® OR could overcome the species barrier to deliver biomolecules between cells of different origin, the BODIPY TR-labeled Exorigin® OR was incubated with HaCaT for 24 h. The result found that Exorigin® OR can interact with cells, as the image showed fluorescence red dots signals of intracellular EVs which were overlapped with the phase contrast of the cells (Figure 1d).

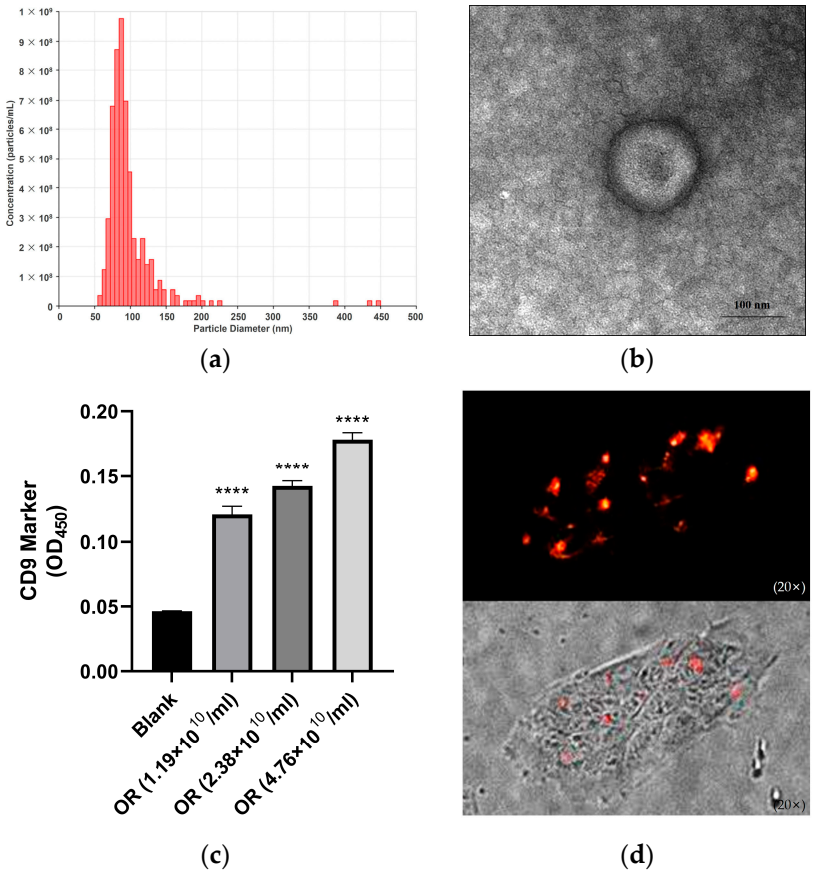

Figure 1. Characterization of Exorigin® OR. (**a**,**b**) Size distribution and morphology of SEC-eluted EVs isolated by qEV platform were examined by Exoid and TEM (30k×). (**c**) CD9 marker was detected by ExoELISA-ULTRA Complete Kit. The data are presented as mean ± SD ($n = 3$) and analyzed using one-way ANOVA with Dunnett's multiple comparisons test. **** $p < 0.0001$ compared with blank. (**d**) Intracellular uptake of BODIPY TR-labeled Exorigin® OR (red dots) was observed by fluorescence microscope (20×) at 24 h after incubation with HaCaT cells.

3.2. Protective Effect of Exorigin® OR Against H_2O_2-Induced Cell Injury

HaCaT cells are a human keratinocyte cell line, and previous studies have shown that they respond to UVB/UVA irradiation or H_2O_2 exposure, resulting in cellular damage and oxidative stress [29]. The protective effect of Exorigin® OR on the viability of HaCaT cells treated with H_2O_2 was detected using MTT assay. The results showed that Exorigin® OR alone did not induce cytotoxic effects at concentrations up to 2.38×10^9/mL (Figure 2a). H_2O_2 induced a decrease in HaCaT cell viability compared with control (100.0 ± 1.5%, $p < 0.0001$). Exorigin® OR pre-treatment increased cell viability from 53.6 ± 1.1% in

the injury group to 56.4 ± 1.4% (non-significant), 58.8 ± 1.1% (non-significant) and 66.4 ± 3.1% ($p < 0.01$), respectively (Figure 2b). The above results are consistent with the images as seen by Sirius Red staining. The group with 2.38 × 10^9/mL of Exorigin® OR has more cells than the H_2O_2-induced group (Figure 2c). These results demonstrate that high content of Exorigin® OR pre-treatment can improve the survival of HaCaT cells exposed to H_2O_2.

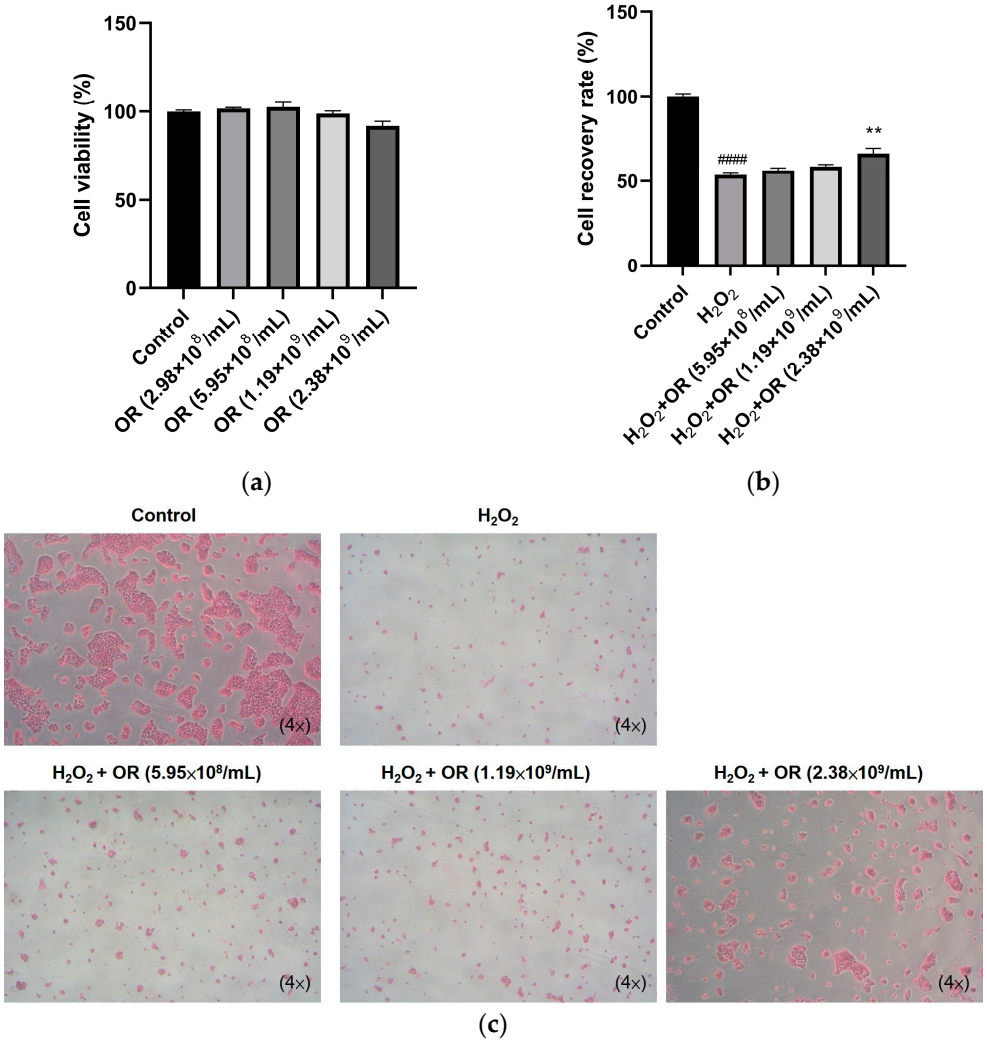

Figure 2. Protective effect of Exorigin® OR against H_2O_2-induced cell injury. (**a**) The effect of Exorigin® OR on the viability of HaCaT was tested after twenty-four-hour treatment by MTT assay. (**b**) HaCaT cells (10^4 cells/well) were pre-treated with different concentrations of Exorigin® OR, then stimulated with H_2O_2 for 24 h. (**c**) The cells were stained with Sirius Red to visualize the cell images (4×). Results were analyzed using one-way ANOVA with Dunnett's multiple comparisons test. #### $p < 0.0001$ compared with Control. ** $p < 0.01$ compared with H_2O_2 group.

3.3. Exorigin® OR Inhibits Melanin Production

Although extracts from Orchidaceae plants have been reported to exhibit anti-melanogenic activity [37], there have been no reports regarding the genus Phalaenopsis. B16-F0 cells are a murine melanoma cell line that can be stimulated through relevant ligand (e.g., α-MSH) to activate the melanogenesis pathway and modulate the expression of genes involved in melanin metabolism [28]. In this study, 3-isobutyl-1-methylxanthine (IBMX), an inhibitor of phosphodiesterase, was used to stimulate the signal pathway of melanogenesis in B16-F0 cells [28]. When B16-F0 cells were incubated with IBMX, the cell pellet turned black, indicating increased cellular melanogenesis (Figure 3a). Exorigin® OR dependently

decreased IBMX-induced melanin production, with significant inhibition observed from the content of 1.19 × 10^8/mL to 4.76 × 10^8/mL (Figure 3b). No cytotoxicity was observed at the same content of Exorigin® OR determined by the MTT assay (Figure 3c). These results demonstrate that Exorigin® OR can effectively inhibit IBMX-induced melanogenesis in B16-F0 cells.

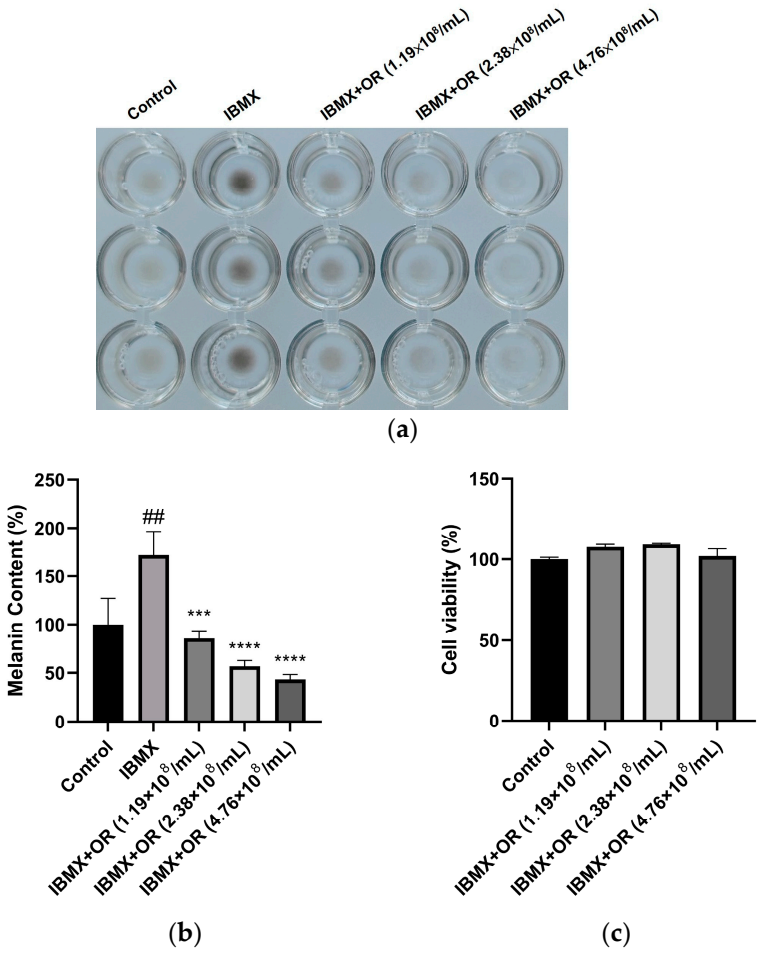

Figure 3. Effect of Exorigin® OR on melanin content and cytotoxicity in B16-F0 cells. (**a**,**b**) Cells were incubated with various concentrations of Exorigin® OR in the presence of IBMX for 4 days. Melanin content was recorded by photograph and absorption of melanin in dissolved cell pellets (**a**,**b**). All viability was determined by MTT assay (**c**). The data are expressed as a percentage of control and presented as mean ± SD (n = 3) and analyzed using one-way ANOVA with Dunnett's multiple comparisons test. ## $p < 0.01$ compared with control. *** $p < 0.001$, **** $p < 0.0001$ compared with induced group.

3.4. Effects of Exorigin® OR on the Expression of Melanin Synthesis-Related Genes

Similarly to the α-MSH-MC1R pathway, IBMX induced MITF-target genes including Mitf Tyr and Tyrp-1 [38]. To study the mechanisms by which Exorigin® OR regulate melanin production, we measured the expression level of each of these genes by Q-PCR analysis. As shown in Figure 4, IBMX treatment increased expression of *Mitf* (1.75-fold), *Tyr* (3.28-fold), and *Tyrp-1* (3.33-fold) compared with the untreated group. Exorigin® OR significantly reduces the expression of the *Tyrp1* gene.

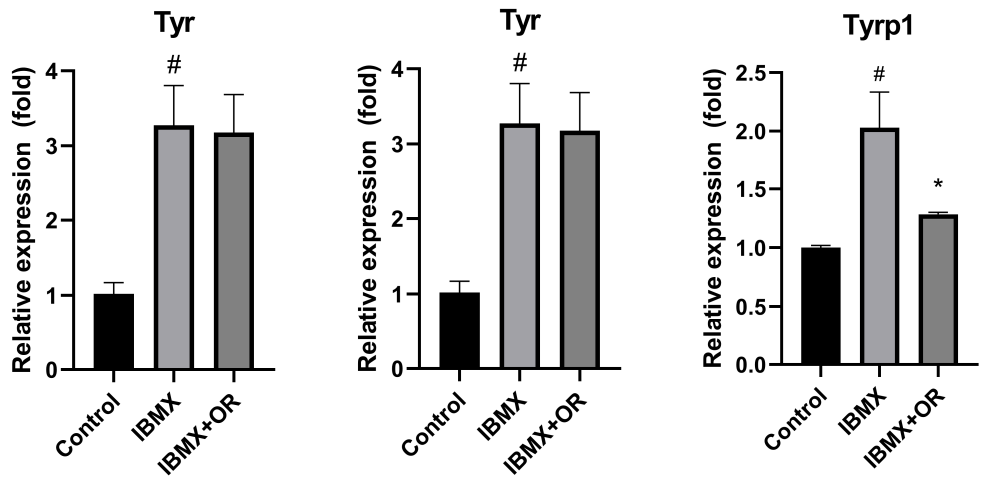

Figure 4. Effect of Exorigin® OR on expression of melanin synthesis-related gene in B16-F0 cells. Cells were incubated with Exorigin® OR (4.76×10^8/mL) in the presence of IBMX for 2 days. Gene expression was analyzed by Q-PCR. The data are analyzed using one-way ANOVA with Dunnett's multiple comparisons test. # $p < 0.05$ compared with control. * $p < 0.05$ compared with IBMX. *Tyr*, tyrosinase; *Tyrp1*, TYR-related protein 1.

3.5. Exorigin® OR Is Non-Irritant

To evaluate the safety of Exorigin® OR for its application as a cosmetic ingredient, alternative in vitro assays were conducted to assess its irritation potential. The results indicated that exposure to a concentration of 2.38×10^9/mL did not affect cell viability in either the reconstructed human epidermis (RHE) (Figure 5a) or the reconstructed human cornea-like epithelium (RhCE) (Figure 5b) models. Exorigin® OR can be considered a non-irritant ingredient.

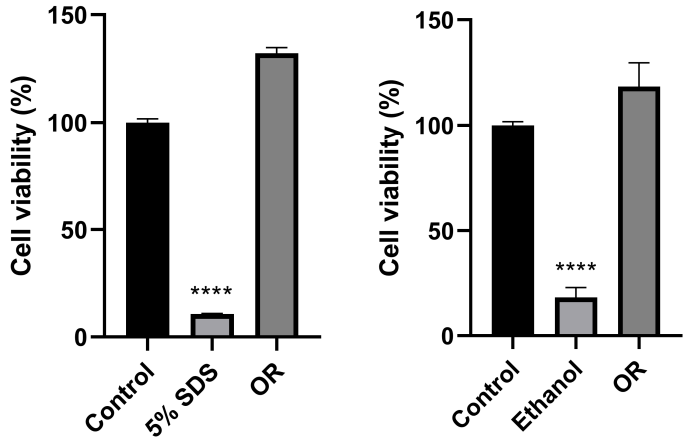

Figure 5. The safety of Exorigin® OR was evaluated using reconstructed skin models. (**a**) In the skin irritation assay, 5% SDS was used as the positive control. (**b**) In the eye irritation assay, ethanol was used as the positive control. Results were analyzed using one-way ANOVA with Dunnett's multiple comparisons test. **** $p < 0.0001$ compared with control.

4. Discussion

In the past five years, the most extensively studied of Orchidaceae for skin care or therapeutic applications include *Dendrobium officinale*, *Dendrobium candidum*, *Bletilla striata*, and *Vanilla pompon*. Extracts derived from these orchids have been shown to exhibit antioxidant [39], wound healing [40], anti-inflammation [41], anti-melanogenesis [39], and anti-aging effects on skin cells [42,43]. These effects may originate from active constituents

contained in plant extracts, including polysaccharides and other phytochemicals. Therefore, Orchidaceae represent promising candidates for cosmetic ingredient development.

In this study, unlike conventional plant extracts, we report for the first time a novel pExo isolated from *P. aphrodite* and investigate its physical and biological properties. Based on our results, the morphology, size, and surface marker of PELVs resemble those of mammalian exosomes. Prior work has detected the surface markers CD9, CD63, and CD81 on grapefruit-derived extracellular vesicles [36]; these tetraspanin proteins play important roles in cross-kingdom communication. Because plants possess CD9 structures similar to those of mammals, we selected CD9 for detection [35]. A limitation of this study is the current lack of antibodies specific to plant CD9; therefore, we used an ELISA kit with antibodies raised against animal CD9. Notably, a dose-dependent detectable signal was observed, suggesting that PAEVs possess features consistent with those of exosomes. In addition, TET8 or TET9 (similarly to CD63) can serve as markers for plant-derived EVs in our future experiments [3].

PELVs have been reported to be internalized by mammalian cells, thereby delivering signals to target cells and modulating cellular functions [44]. Given the lipid bilayer enriched in sphingomyelin and ceramide, we labeled the Exorigin® OR with BODIPY™ TR ceramide dye and incubated them with keratinocytes. Fluorescence microscopy revealed punctate signals in cells, suggesting vesicle engage keratinocytes via membrane contact and/or internalization; however, internalization would need to be further confirmed using endocytic inhibitors [45]. Previous studies have reported that PELVs exhibit various biological activities in in vitro and in vivo models, which may confer potential health benefits to humans. For example, grapefruit-derived nanovesicles ameliorate dextran sulfate sodium (DSS)-induced mouse colitis [46]. Ginseng root-derived exosome-like nanoparticles have been shown to protect keratinocytes against UV- and H_2O_2-induced damage and inflammation, suggesting their potential as skin-protective agents [29]. In addition, extracellular vesicles isolated from the leaves and stems of *Dendropanax morbifera* show inhibitory effects on melanogenesis in mouse melanoma cells [47]. According to the current literature, two studies have reported that Phalaenopsis orchid extracts can inhibit fibroblast senescence and suppress melanogenesis. Water extract of Phalaenopsis orchid flower (WEPF) counteracts ROS-induced fibroblast senescence by activating the Nrf2/HO-1 axis under high glucose-induced stress [48]. Similarly, as a water extract, it can suppress WNT1-induced differentiation of melanocyte stem cells, thereby suggesting potential applicability in solar lentigines [49]. Therefore, our study focused on the protective effects of PELVs on skin cells and their potential to inhibit melanin synthesis.

External environmental factors, such as ultraviolet (UV) radiation from sunlight, can significantly affect skin health. UV exposure induces the generation of reactive oxygen species (ROS) in the skin (e.g., hydrogen peroxide, singlet oxygen, and hydroxyl radicals), which in turn trigger autophagy, reduce the activity of antioxidant-related enzymes, and damage intracellular structural proteins [50]. UV-induced ROS generation also leads to increased melanogenesis [51]. These effects ultimately lead to skin dryness, functional impairment, hyperpigmentation, and an increased risk of skin disorders. The results of this study revealed that Exorigin® OR can attenuate H_2O_2-induced damage in keratinocytes, inhibit melanin production in melanocytes and exhibits ABTS radical-scavenging activity (Appendix A). Interestingly, compared with the concentrations used in the cell damage model, lower concentrations of Exorigin® OR already exhibited notable anti-melanogenic activity. This concentration-dependent difference may be attributed to distinct cellular responses or regulatory mechanisms involved in keratinocytes and melanocytes.

The unexpected observation that lower concentrations of Exorigin® OR exerted stronger effects on melanocytes led us to perform a preliminary study to elucidate the

possible mechanisms involved. Melanogenesis is initiated by the binding of α-melanocyte-stimulating hormone (α-MSH) to its receptor, activating G protein-coupled receptor (GPCR) signaling. This stimulation enhances adenylyl cyclase activity, elevating intracellular cAMP and activating protein kinase A (PKA). PKA phosphorylates CREB, which induces microphthalmia-associated transcription factor (*Mitf*) expression to regulate melanogenic enzymes such as tyrosinase (*Tyr*) and tyrosinase-related proteins (*Tyrp1/2*). IBMX is a phosphodiesterase inhibitor, which can increase intracellular cAMP levels [28]. In this study, consistent with previous findings [52], IBMX induced melanogenesis and upregulated the expression of *Mitf*, *Tyr*, and *Tyrp1* genes. Interestingly, although Exorigin® OR suppressed melanin production, they inhibited only the expression of *Tyrp1* but not *Tyr* after two days treatment. The observed selective inhibition may be associated with the regulatory mechanism of the *Tyrp* gene promoter. It is speculated that certain inhibitory factors might selectively interfere with the binding of MITF to the M box element, thereby modulating transcriptional activity [53]. To our knowledge, one study has reported that AKT can phosphorylate MITF, thereby promoting its association with ID4 and concomitantly suppressing TYR expression [54]; however, no repressor protein has been reported to selectively regulate *Tyrp1* gene expression. Alternatively, it is possible that reductions in *Tyr* or *Mitf* expression may occur at different time points. In other words, changes in the expression of different genes may not occur simultaneously, and additional time-course experiments will be required to validate this hypothesis. Furthermore, previous pulse-chase studies demonstrated that tyrosinase is degraded more rapidly in *Tyrp1* mutant melanocytes and that reintroduction of wild-type *Tyrp1* partially rescues tyrosinase stability, indicating that TYRP1 can modulate the turnover of TYR [55]. Collectively, these findings suggest that Exorigin® OR may play a role in cellular regulatory processes; however, their precise mechanisms of action remain to be elucidated. Further investigations are required to determine whether Exorigin® OR participate directly in these pathways.

In addition, the miRNAs enclosed within the vesicles may serve as potential mediators of their biological effects. The microRNA (miRNA) transcriptome of *P. aphrodite* has been elucidated, providing a valuable resource for mechanistic studies [24]. Accordingly, future investigations may examine whether Exorigin® OR influence melanogenesis by modulating specific gene expression or protein translation via miRNA-dependent pathways.

Residual co-isolated substances generated during extracellular vesicle (EV) preparation may confound the outcomes observed in anti-melanogenic assays. Although the chemical composition of Exorigin® OR has not yet been characterized, a previous study reported that extracts from white flowers of *P. aphrodite* primarily contain gallic acid, p-coumaric acid, and quercitrin [56]. Using the reported dry-weight proportions of these compounds, we estimated their putative levels in Exorigin® OR based on its dry weight, converted these estimates to the corresponding concentrations under our assay conditions, and compared them with bioactive concentrations reported in the literature [57–59]. Notably, the estimated concentrations of gallic acid, p-coumaric acid, and quercitrin in cell model were substantially lower than those reported to inhibit melanogenesis (approximately 67.2-, 217.3-, and 44.3-fold lower, respectively), suggesting that these individual compounds are unlikely to account for the anti-melanogenic effects of the result. Given that previous studies have suggested that EVs can encapsulate plant-derived small-molecule compounds [60,61], we cannot exclude the possibility that Phalaenopsis-derived exosome-like EVs may also carry its unique phytochemicals.

With regard to safety, our results demonstrate that Exorigin® OR does not exhibit acute irritation potential. Additional alternative in vitro assays are required to further evaluate the possibility of sensitization following long-term exposure. Importantly, to date, no reports have specifically implicated *P. aphrodite* in such adverse effects.

In conclusion, we isolated, purified, and characterized exosome-like nanoparticles from *P. aphrodite*. These PELVs may be internalized by keratinocytes, thereby exerting protective effects against oxidative stress-induced skin cell damage, and may also exhibit anti-melanogenic activity in melanocytes. Our preliminary mechanistic findings suggest that these effects may be associated with reduced *Tyrp1* gene expression; however, further studies are required to elucidate the upstream regulatory mechanisms, relevant post-translational processes, and the potential targets of vesicle-contained miRNAs in mammalian cells. Moreover, alternative testing confirmed that Exorigin® OR is non-irritant. Collectively, these findings provide new insights into the beneficial potential of *P. aphrodite* and suggest that its exosome-like extracellular vesicles may serve as promising and safe bioactive ingredients for promoting skin health in cosmeceutical applications.

Author Contributions: Conceptualization, K.-C.L. and K.-A.C.; methodology, H.-J.Y., P.-Y.T., I.H.L., C.H.L. and K.-A.C.; software, K.-A.C.; validation, H.-J.Y., P.-Y.T. and K.-A.C.; formal analysis, K.-A.C.; investigation, K.-C.L. and K.-A.C.; resources, H.-J.Y.; data curation, K.-A.C., H.-J.Y. and P.-Y.T.; writing—original draft preparation, K.-A.C., H.-J.Y. and P.-Y.T.; writing—review and editing, K.-A.C., C.-C.L. and H.U.; visualization, K.-A.C.; supervision, I.-H.P.; project administration, K.-C.L.; funding acquisition, I.-H.P. and K.-C.L. All authors have read and agreed to the published version of the manuscript.

Funding: This research was supported by the R&D budget of Pegavision Corp.

Institutional Review Board Statement: Not applicable.

Informed Consent Statement: Not applicable.

Data Availability Statement: The original contributions presented in this study are included in the article.

Acknowledgments: We gratefully acknowledge the Industrial Technology Research Institute (ITRI) for their assistance in plant material preparation. Additionally, we would like to thank C.C. Lin and H. Umbreen for their efforts in reviewing the manuscript.

Conflicts of Interest: Author Kai-An Chuang, Kuei-Chang Li, Hsin-Jan Yao, Pei-Yin Tsai and I-Hong Pan were employed by the company Advanced Product R&D Center, Pegavision Corp. and FacialBeau International Corp. The remaining authors declare that the research was conducted in the absence of any commercial or financial relationships that could be construed as a potential conflict of interest.

Abbreviations

The following abbreviations are used in this manuscript:

IBMX	3-isobutyl-1-methylxanthine
PELVs	Plant-derived exosome-like extracellular vesicles
pExo	Plant-derived exosomes
RHE	Reconstructed human epidermis
RhCE	Reconstructed human cornea-like epithelium
ROS	Reactive oxygen species
Tyrp-1	TYR-related protein 1
TFF	Tangential flow filtration

Appendix A

Table A1. Antioxidant activity of Exorigin® OR by ABTS and DPPH radicals assays.

Sample	Concentration	Scavenging Activity (%)	
		ABTS	DPPH
Vitamin C	15.6 (µg/mL)	10.7 ± 0.1	2.3 ± 4.4
	31.3 (µg/mL)	17.9 ± 0.1	9.4 ± 5.1
	62.5 (µg/mL)	33.3 ± 0.2	21.3 ± 4.4
	125.0 (µg/mL)	94.8 ± 0.9	42.2 ± 4.1
	250.0 (µg/mL)	95.8 ± 0.0	83.4 ± 3.8
Exorigin® OR	1.19×10^8 (Particles/mL)	27.5 ± 1.0	No activity
	2.38×10^8 (Particles/mL)	52.0 ± 0.1	No activity
	4.76×10^8 (Particles/mL)	96.0 ± 2.9	No activity

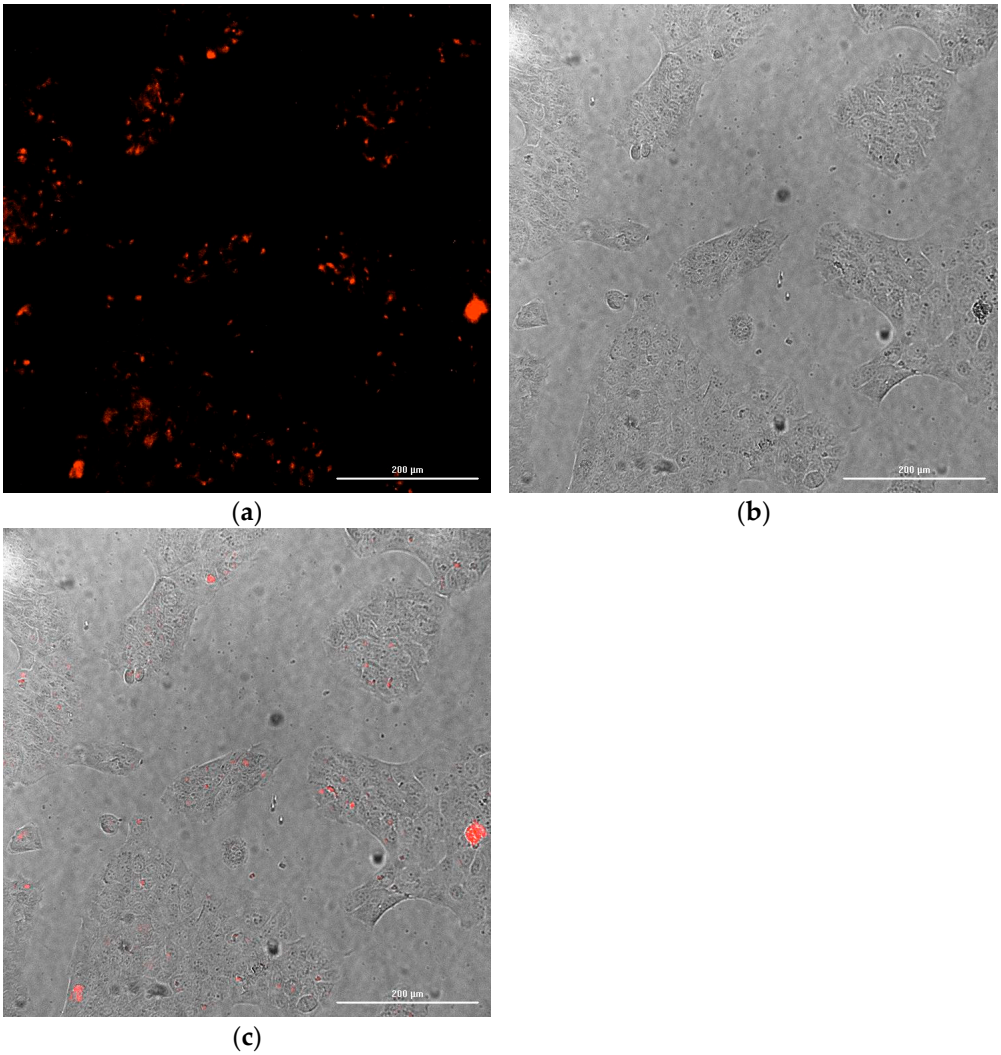

(**a**) (**b**)

(**c**)

Figure A1. Original data of fluorescence microscopy (**a**), phase contrast (**b**) and merged images analysis (**c**) of HaCaT cells incubated for 24 h with BODIPY TR ceramide labeled Exorigin® OR. Photographs were taken at a magnification of 20×.

References

1. Lian, M.Q.; Chng, W.H.; Liang, J.; Yeo, H.Q.; Lee, C.K.; Belaid, M.; Tollemeto, M.; Wacker, M.G.; Czarny, B.; Pastorin, G. Plant-Derived Extracellular Vesicles: Recent Advancements and Current Challenges on Their Use for Biomedical Applications. *J. Extracell. Vesicles* **2022**, *11*, e12283. [CrossRef]

2. An, Q.; van Bel, A.J.; Hückelhoven, R. Do Plant Cells Secrete Exosomes Derived from Multivesicular Bodies? *Plant Signal. Behav.* **2007**, *2*, 4–7. [CrossRef]
3. Zhao, B.; Lin, H.; Jiang, X.; Li, W.; Gao, Y.; Li, M.; Yu, Y.; Chen, N.; Gao, J. Exosome-like Nanoparticles Derived from Fruits, Vegetables, and Herbs: Innovative Strategies of Therapeutic and Drug Delivery. *Theranostics* **2024**, *14*, 4598–4621. [CrossRef] [PubMed]
4. Zhan, W.; Deng, M.; Huang, X.; Xie, D.; Gao, X.; Chen, J.; Shi, Z.; Lu, J.; Lin, H.; Li, P. Pueraria Lobata-Derived Exosome-like Nanovesicles Alleviate Osteoporosis by Enhacning Autophagy. *J. Control. Release* **2023**, *364*, 644–653. [CrossRef]
5. Chen, Q.; Zu, M.; Gong, H.; Ma, Y.; Sun, J.; Ran, S.; Shi, X.; Zhang, J.; Xiao, B. Tea Leaf-Derived Exosome-like Nanotherapeutics Retard Breast Tumor Growth by pro-Apoptosis and Microbiota Modulation. *J. Nanobiotechnol.* **2023**, *21*, 6. [CrossRef]
6. Kilasoniya, A.; Garaeva, L.; Shtam, T.; Spitsyna, A.; Putevich, E.; Moreno-Chamba, B.; Salazar-Bermeo, J.; Komarova, E.; Malek, A.; Valero, M.; et al. Potential of Plant Exosome Vesicles from Grapefruit (*Citrus* × *Paradisi*) and Tomato (*Solanum lycopersicum*) Juices as Functional Ingredients and Targeted Drug Delivery Vehicles. *Antioxidants* **2023**, *12*, 943. [CrossRef]
7. Li, M.; Chen, T.; Wang, R.; Luo, J.-Y.; He, J.-J.; Ye, R.-S.; Xie, M.-Y.; Xi, Q.-Y.; Jiang, Q.-Y.; Sun, J.-J.; et al. Plant MIR156 Regulates Intestinal Growth in Mammals by Targeting the Wnt/β-Catenin Pathway. *Am. J. Physiol. Cell Physiol.* **2019**, *317*, C434–C448. [CrossRef]
8. Baker, P.; Huang, C.; Radi, R.; Moll, S.B.; Jules, E.; Arbiser, J.L. Skin Barrier Function: The Interplay of Physical, Chemical, and Immunologic Properties. *Cells* **2023**, *12*, 2745. [CrossRef] [PubMed]
9. Bos, J.D.; Meinardi, M.M. The 500 Dalton Rule for the Skin Penetration of Chemical Compounds and Drugs. *Exp. Dermatol.* **2000**, *9*, 165–169. [CrossRef] [PubMed]
10. Yepes-Molina, L.; Martínez-Ballesta, M.C.; Carvajal, M. Plant Plasma Membrane Vesicles Interaction with Keratinocytes Reveals Their Potential as Carriers. *J. Adv. Res.* **2020**, *23*, 101–111. [CrossRef]
11. Hou, J.; Wei, W.; Geng, Z.; Zhang, Z.; Yang, H.; Zhang, X.; Li, L.; Gao, Q. Developing Plant Exosomes as an Advanced Delivery System for Cosmetic Peptide. *ACS Appl. Bio Mater.* **2024**, *7*, 3050–3060. [CrossRef] [PubMed]
12. Wei, W.; Ren, X.; Yi, F.; Zhang, X.; Hou, J.; Zhang, Z.; Yuan, L.; Li, L.; Gao, Q. Innovative Plant Exosome Delivery System for Enhancing Antiaging Potency on Skin. *ACS Appl. Bio Mater.* **2025**, *8*, 2117–2127. [CrossRef]
13. Dad, H.A.; Gu, T.-W.; Zhu, A.-Q.; Huang, L.-Q.; Peng, L.-H. Plant Exosome-like Nanovesicles: Emerging Therapeutics and Drug Delivery Nanoplatforms. *Mol. Ther. J. Am. Soc. Gene Ther.* **2021**, *29*, 13–31. [CrossRef]
14. Bai, C.; Liu, J.; Zhang, X.; Li, Y.; Qin, Q.; Song, H.; Yuan, C.; Huang, Z. Research Status and Challenges of Plant-Derived Exosome-like Nanoparticles. *Biomed. Pharmacother.* **2024**, *174*, 116543. [CrossRef] [PubMed]
15. Hadi, H.; Razali, S.N.S.; Awadh, A.I. A Comprehensive Review of the Cosmeceutical Benefits of *Vanda* Species (Orchidaceae). *Nat. Prod. Commun.* **2015**, *10*, 1483–1488. [CrossRef] [PubMed]
16. Bulpitt, C.J.; Li, Y.; Bulpitt, P.F.; Wang, J. The Use of Orchids in Chinese Medicine. *J. R. Soc. Med.* **2007**, *100*, 558–563. [CrossRef]
17. Simmler, C.; Antheaume, C.; André, P.; Bonté, F.; Lobstein, A. Glucosyloxybenzyl Eucomate Derivatives from Vanda Teres Stimulate HaCaT Cytochrome c Oxidase. *J. Nat. Prod.* **2011**, *74*, 949–955. [CrossRef]
18. Simmler, C.; Antheaume, C.; Lobstein, A. Antioxidant Biomarkers from Vanda Coerulea Stems Reduce Irradiated HaCaT PGE-2 Production as a Result of COX-2 Inhibition. *PLoS ONE* **2010**, *5*, e13713. [CrossRef]
19. Andre, P.; Archambault, J.-C.; Renimel, I. Use of an Extract of the Orchid as a Skin Hydrating Agent Patent. U.S. Patent 8,039,028, 18 October 2011. Available online: https://patents.justia.com/patent/8039028 (accessed on 14 November 2025).
20. Peng, P.-H.; Lin, C.-H.; Tsai, H.-W.; Lin, T.-Y. Cold Response in *Phalaenopsis aphrodite* and Characterization of PaCBF1 and PaICE1. *Plant Cell Physiol.* **2014**, *55*, 1623–1635. [CrossRef]
21. Lou, Y.; Zhang, Q.; Xu, Q.; Yu, X.; Wang, W.; Gai, R.; Ming, F. PhCHS5 and PhF3′5′H Genes Over-Expression in *Petunia* (*Petunia hybrida*) and *Phalaenopsis* (*Phalaenopsis aphrodite*) Regulate Flower Color and Branch Number. *Plants* **2023**, *12*, 2204. [CrossRef]
22. Ho, B.-L.; Chen, J.-C.; Huang, T.-P.; Fang, S.-C. Protocorm-like-Body Extract of *Phalaenopsis aphrodite* Combats Watermelon Fruit Blotch Disease. *Front. Plant Sci.* **2022**, *13*, 1054586. [CrossRef] [PubMed]
23. Sun, W.-T.; Cheng, S.-C.; Chao, Y.-T.; Lin, S.-Y.; Yang, T.-T.; Ho, Y.-P.; Shih, M.-C.; Ko, S.-S. Sugars and Sucrose Transporters in Pollinia of *Phalaenopsis aphrodite* (*Orchidaceae*). *J. Exp. Bot.* **2023**, *74*, 2556–2571. [CrossRef] [PubMed]
24. Chao, Y.-T.; Su, C.-L.; Jean, W.-H.; Chen, W.-C.; Chang, Y.-C.A.; Shih, M.-C. Identification and Characterization of the microRNA Transcriptome of a Moth Orchid *Phalaenopsis aphrodite*. *Plant Mol. Biol.* **2014**, *84*, 529–548. [CrossRef]
25. Trentini, M.; Zanolla, I.; Zanotti, F.; Tiengo, E.; Licastro, D.; Dal Monego, S.; Lovatti, L.; Zavan, B. Apple Derived Exosomes Improve Collagen Type I Production and Decrease MMPs during Aging of the Skin through Downregulation of the NF-κB Pathway as Mode of Action. *Cells* **2022**, *11*, 3950. [CrossRef]
26. Perut, F.; Roncuzzi, L.; Avnet, S.; Massa, A.; Zini, N.; Sabbadini, S.; Giampieri, F.; Mezzetti, B.; Baldini, N. Strawberry-Derived Exosome-Like Nanoparticles Prevent Oxidative Stress in Human Mesenchymal Stromal Cells. *Biomolecules* **2021**, *11*, 87. [CrossRef]
27. Yang, J.; Celebi, L.E.; Hawthorne, L.; Ozcebe, S.G.; Zorlutuna, P. Substrate Stiffness Modulates Fibroblast Extracellular Vesicle Secretion Via Mechanotransduction Pathways. *Small* **2025**, *21*, e05261. [CrossRef]

28. Koo, J.-H.; Kim, H.T.; Yoon, H.-Y.; Kwon, K.-B.; Choi, I.-W.; Jung, S.H.; Kim, H.-U.; Park, B.-H.; Park, J.-W. Effect of Xanthohumol on Melanogenesis in B16 Melanoma Cells. *Exp. Mol. Med.* **2008**, *40*, 313–319. [CrossRef]
29. Choi, W.; Cho, J.H.; Park, S.H.; Kim, D.S.; Lee, H.P.; Kim, D.; Kim, H.S.; Kim, J.H.; Cho, J.Y. Ginseng Root-Derived Exosome-like Nanoparticles Protect Skin from UV Irradiation and Oxidative Stress by Suppressing Activator Protein-1 Signaling and Limiting the Generation of Reactive Oxygen Species. *J. Ginseng Res.* **2024**, *48*, 211–219. [CrossRef]
30. Abel, F.; Murke, F.; Gaida, M.; Garnier, N.; Ochsenfarth, C.; Theiss, C.; Thielmann, M.; Kleinbongard, P.; Giebel, B.; Peters, J.; et al. Extracellular Vesicles Isolated from Patients Undergoing Remote Ischemic Preconditioning Decrease Hypoxia-Evoked Apoptosis of Cardiomyoblasts after Isoflurane but Not Propofol Exposure. *PLoS ONE* **2020**, *15*, e0228948. [CrossRef] [PubMed]
31. Wu, S.-Y.S.; Wang, H.-M.D.; Wen, Y.-S.; Liu, W.; Li, P.-H.; Chiu, C.-C.; Chen, P.-C.; Huang, C.-Y.; Sheu, J.-H.; Wen, Z.-H. 4-(Phenylsulfanyl)Butan-2-One Suppresses Melanin Synthesis and Melanosome Maturation In Vitro and In Vivo. *Int. J. Mol. Sci.* **2015**, *16*, 20240–20257. [CrossRef]
32. Zhang, J.; Ye, Z.; Bräutigam, L.; Chakraborty, P.; Luo, Z.; Culpepper, J.; Aslam, M.; Zhang, L.; Johansson, K.; Haeggström, J.Z.; et al. A Role for Microsomal Glutathione Transferase 1 in Melanin Biosynthesis and Melanoma Progression. *J. Biol. Chem.* **2023**, *299*, 104920. [CrossRef]
33. Qomaladewi, N.P.; Kim, M.-Y.; Cho, J.Y. Rottlerin Reduces cAMP/CREB-Mediated Melanogenesis via Regulation of Autophagy. *Int. J. Mol. Sci.* **2019**, *20*, 2081. [CrossRef] [PubMed]
34. Welsh, J.A.; Goberdhan, D.C.I.; O'Driscoll, L.; Buzas, E.I.; Blenkiron, C.; Bussolati, B.; Cai, H.; Di Vizio, D.; Driedonks, T.A.P.; Erdbrügger, U.; et al. Minimal Information for Studies of Extracellular Vesicles (MISEV2023): From Basic to Advanced Approaches. *J. Extracell. Vesicles* **2024**, *13*, e12404. [CrossRef]
35. Jimenez-Jimenez, S.; Hashimoto, K.; Santana, O.; Aguirre, J.; Kuchitsu, K.; Cárdenas, L. Emerging Roles of Tetraspanins in Plant Inter-Cellular and Inter-Kingdom Communication. *Plant Signal. Behav.* **2019**, *14*, e1581559. [CrossRef] [PubMed]
36. Savcı, Y.; Kırbaş, O.K.; Bozkurt, B.T.; Abdik, E.A.; Taşlı, P.N.; Şahin, F.; Abdik, H. Grapefruit-Derived Extracellular Vesicles as a Promising Cell-Free Therapeutic Tool for Wound Healing. *Food Funct.* **2021**, *12*, 5144–5156. [CrossRef]
37. Chan, C.-F.; Wu, C.-T.; Huang, W.-Y.; Lin, W.-S.; Wu, H.-W.; Huang, T.-K.; Chang, M.-Y.; Lin, Y.-S. Antioxidation and Melanogenesis Inhibition of Various Dendrobium Tosaense Extracts. *Molecules* **2018**, *23*, 1810. [CrossRef]
38. Han, S.-Y.; Jang, T.-W.; Park, H.-J.; Oh, S.-S.; Lee, J.-B.; Myoung, S.-M.; Park, J.-H. *Nypa fruticans* Wurmb Inhibits Melanogenesis in Isobutylmethylxanthine-treated Melanoma via the PI3K/AKT/mTOR/CREB and MAPK Signaling Pathways. *Exp. Ther. Med.* **2022**, *24*, 754. [CrossRef] [PubMed]
39. Chen, H.; Wu, Y.; Wang, B.; Kui, M.; Xu, J.; Ma, H.; Li, J.; Zeng, J.; Gao, W.; Chen, K. Skin Healthcare Protection with Antioxidant and Anti-Melanogenesis Activity of Polysaccharide Purification from *Bletilla striata*. *Int. J. Biol. Macromol.* **2024**, *262*, 130016. [CrossRef]
40. Li, J.; Zhao, Q.; Gao, X.; Dai, T.; Bai, Z.; Sheng, J.; Tian, Y.; Bai, Z. Dendrobium Officinale Kinura et Migo Glycoprotein Promotes Skin Wound Healing by Regulating Extracellular Matrix Secretion and Fibroblast Proliferation on the Proliferation Phase. *Wound Repair Regen.* **2024**, *32*, 55–66. [CrossRef]
41. Zeng, B.; Yan, Y.; Zhang, Y.; Wang, C.; Huang, W.; Zhong, X.; Chen, Z.; Xie, M.; Yang, Z. Dendrobium Officinale Polysaccharide (DOP) Inhibits Cell Hyperproliferation, Inflammation and Oxidative Stress to Improve Keratinocyte Psoriasis-like State. *Adv. Med. Sci.* **2024**, *69*, 167–175. [CrossRef]
42. Guo, L.; Yang, Y.; Pu, Y.; Mao, S.; Nie, Y.; Liu, Y.; Jiang, X. Dendrobium Officinale Kimura & Migo Polysaccharide and Its Multilayer Emulsion Protect Skin Photoaging. *J. Ethnopharmacol.* **2024**, *318*, 116974. [CrossRef]
43. Zhou, H.; Zhou, L.; Li, B.; Yue, R. Anti-Cyclooxygenase, Anti-Glycation, and Anti-Skin Aging Effect of *Dendrobium officinale* Flowers' Aqueous Extract and Its Phytochemical Validation in Aging. *Front. Immunol.* **2023**, *14*, 1095848. [CrossRef]
44. Gupta, R.; Gupta, S.; Gupta, P.; Nüssler, A.K.; Kumar, A. Establishing the Callus-Based Isolation of Extracellular Vesicles from *Cissus quadrangularis* and Elucidating Their Role in Osteogenic Differentiation. *J. Funct. Biomater.* **2023**, *14*, 540. [CrossRef]
45. Tian, T.; Zhu, Y.-L.; Zhou, Y.-Y.; Liang, G.-F.; Wang, Y.-Y.; Hu, F.-H.; Xiao, Z.-D. Exosome Uptake through Clathrin-Mediated Endocytosis and Macropinocytosis and Mediating miR-21 Delivery. *J. Biol. Chem.* **2014**, *289*, 22258–22267. [CrossRef]
46. Wang, B.; Zhuang, X.; Deng, Z.-B.; Jiang, H.; Mu, J.; Wang, Q.; Xiang, X.; Guo, H.; Zhang, L.; Dryden, G.; et al. Targeted Drug Delivery to Intestinal Macrophages by Bioactive Nanovesicles Released from Grapefruit. *Mol. Ther. J. Am. Soc. Gene Ther.* **2014**, *22*, 522–534. [CrossRef] [PubMed]
47. Lee, R.; Ko, H.J.; Kim, K.; Sohn, Y.; Min, S.Y.; Kim, J.A.; Na, D.; Yeon, J.H. Anti-Melanogenic Effects of Extracellular Vesicles Derived from Plant Leaves and Stems in Mouse Melanoma Cells and Human Healthy Skin. *J. Extracell. Vesicles* **2020**, *9*, 1703480. [CrossRef]
48. Peng, S.-L.; Tsai, C.-M.; Weng, C.-J.; Yang, S.-F. Phalaenopsis Orchid Flower Extract Attenuates High Glucose-Induced Senescence via Nrf2/HO-1 Activation and Promotes Wound Healing in Human Dermal Fibroblasts. *Cell. Mol. Biol.* **2025**, *71*, 110–118. [CrossRef] [PubMed]

49. Yamada, T.; Hasegawa, S.; Inoue, Y.; Kunita, M.; Ohsumi, K.; Sakaida, T.; Yashiro, Y.; Nakata, S. Inhibitory Effect of Phalaenopsis Orchid Extract on WNT1-Induced Immature Melanocyte Precursor Differentiation in a Novel In Vitro Solar Lentigo Model. *Biosci. Biotechnol. Biochem.* **2016**, *80*, 1321–1326. [CrossRef] [PubMed]
50. Chen, J.; Liu, Y.; Zhao, Z.; Qiu, J. Oxidative Stress in the Skin: Impact and Related Protection. *Int. J. Cosmet. Sci.* **2021**, *43*, 495–509. [CrossRef]
51. Gromkowska-Kępka, K.J.; Puścion-Jakubik, A.; Markiewicz-Żukowska, R.; Socha, K. The Impact of Ultraviolet Radiation on Skin Photoaging—Review of In Vitro Studies. *J. Cosmet. Dermatol.* **2021**, *20*, 3427–3431. [CrossRef]
52. Han, H.J.; Park, S.K.; Kang, J.Y.; Kim, J.M.; Yoo, S.K.; Heo, H.J. Anti-Melanogenic Effect of Ethanolic Extract of Sorghum Bicolor on IBMX-Induced Melanogenesis in B16/F10 Melanoma Cells. *Nutrients* **2020**, *12*, 832. [CrossRef]
53. Fang, D.; Tsuji, Y.; Setaluri, V. Selective Down-Regulation of Tyrosinase Family Gene TYRP1 by Inhibition of the Activity of Melanocyte Transcription Factor, MITF. *Nucleic Acids Res.* **2002**, *30*, 3096–3106. [CrossRef]
54. Wang, C.; Zhao, L.; Su, Q.; Fan, X.; Wang, Y.; Gao, S.; Wang, H.; Chen, H.; Chan, C.B.; Liu, Z. Phosphorylation of MITF by AKT Affects Its Downstream Targets and Causes TP53-Dependent Cell Senescence. *Int. J. Biochem. Cell Biol.* **2016**, *80*, 132–142. [CrossRef]
55. Kobayashi, T.; Imokawa, G.; Bennett, D.C.; Hearing, V.J. Tyrosinase Stabilization by Tyrp1 (the Brown Locus Protein). *J. Biol. Chem.* **1998**, *273*, 31801–31805. [CrossRef]
56. Meléndez-Martínez, A.J.; Benítez, A.; Corell, M.; Hernanz, D.; Mapelli-Brahm, P.; Stinco, C.; Coyago-Cruz, E. Screening for Innovative Sources of Carotenoids and Phenolic Antioxidants among Flowers. *Foods* **2021**, *10*, 2625. [CrossRef]
57. Su, T.-R.; Lin, J.-J.; Tsai, C.-C.; Huang, T.-K.; Yang, Z.-Y.; Wu, M.-O.; Zheng, Y.-Q.; Su, C.-C.; Wu, Y.-J. Inhibition of Melanogenesis by Gallic Acid: Possible Involvement of the PI3K/Akt, MEK/ERK and Wnt/β-Catenin Signaling Pathways in B16F10 Cells. *Int. J. Mol. Sci.* **2013**, *14*, 20443–20458. [CrossRef] [PubMed]
58. An, S.M.; Koh, J.; Boo, Y.C. *P*-coumaric Acid Not Only Inhibits Human Tyrosinase Activity In Vitro but Also Melanogenesis in Cells Exposed to UVB. *Phytother. Res.* **2010**, *24*, 1175–1180. [CrossRef] [PubMed]
59. Hong, C.-O.; Lee, H.A.; Rhee, C.H.; Choung, S.-Y.; Lee, K.-W. Separation of the Antioxidant Compound Quercitrin from *Lindera obtusiloba* Blume and Its Antimelanogenic Effect on B16F10 Melanoma Cells. *Biosci. Biotechnol. Biochem.* **2013**, *77*, 58–64. [CrossRef]
60. Stanly, C.; Alfieri, M.; Ambrosone, A.; Leone, A.; Fiume, I.; Pocsfalvi, G. Grapefruit-Derived Micro and Nanovesicles Show Distinct Metabolome Profiles and Anticancer Activities in the A375 Human Melanoma Cell Line. *Cells* **2020**, *9*, 2722. [CrossRef] [PubMed]
61. Guo, Z.; Li, G.; Shen, L.; Pan, J.; Dou, D.; Gong, Y.; Shi, W.; Sun, Y.; Zhang, Y.; Ma, K.; et al. Ginger-Derived Exosome-like Nanoparticles Loaded with Indocyanine Green Enhances Phototherapy Efficacy for Breast Cancer. *Int. J. Nanomed.* **2025**, *20*, 1147–1169. [CrossRef]

Disclaimer/Publisher's Note: The statements, opinions and data contained in all publications are solely those of the individual author(s) and contributor(s) and not of MDPI and/or the editor(s). MDPI and/or the editor(s) disclaim responsibility for any injury to people or property resulting from any ideas, methods, instructions or products referred to in the content.